

Properties of a thin accretion disk around a rotating non-Kerr black hole

Songbai Chen^{*}, Jiliang Jing[†]

*Institute of Physics and Department of Physics, Hunan Normal University,
Changsha, Hunan 410081, People's Republic of China
Key Laboratory of Low Dimensional Quantum Structures
and Quantum Control of Ministry of Education, Hunan Normal University,
Changsha, Hunan 410081, People's Republic of China*

Abstract

We study the accretion process in the thin disk around a rotating non-Kerr black hole with a deformed parameter and an unbound rotation parameter. Our results show that the presence of the deformed parameter ϵ modifies the standard properties of the disk. For the case in which the black hole is more oblate than a Kerr black hole, the larger deviation leads to the smaller energy flux, the lower radiation temperature and the fainter spectra luminosity in the disk. For the black hole with positive deformed parameter, we find that the effect of the deformed parameter on the disk becomes more complicated. It depends not only on the rotation direction of the black hole and the orbit particles, but also on the sign of the difference between the deformed parameter ϵ and a certain critical value ϵ_c . These significant features in the mass accretion process may provide a possibility to test gravity in the strong field regime in future astronomical observations.

PACS numbers: 04.70.Dy, 95.30.Sf, 97.60.Lf

^{*} csb3752@163.com

[†] jljing@hunnu.edu.cn

I. INTRODUCTION

General relativity is the simplest theory of gravity and is consistent with the current experimental data. In general relativity, a neutral rotating black hole in asymptotically flat and matter-free spacetime is described completely by the Kerr metric only with two parameters, the mass M and the rotation parameter a , which is supported by the well-known no-hair theorem [1]. For a Kerr black hole with $a > M$, the event horizon vanishes and the central singularity is naked, which is forbidden by the weak cosmic censorship conjecture [2]. Thus, it seems to be doomed to fail to get a naked singularity through over-spinning Kerr black hole in general relativity [3]. However, it is argued that general relativity has been tested only for weak gravitational fields [4]. In the strong gravity regime, general relativity could be broken down and astrophysical black holes might not be Kerr black holes as predicted by the no-hair theorem [5–7].

In order to test gravity in the strong field regime, Johannsen *et al* [6] applied recently the Newman-Janis transformation [8] and constructed a deformed Kerr-like metric, which describes a rotating black hole beyond general relativity. The nature of the alternative theory of gravity describing this rotating black hole is unclear at present. Besides the mass M and the rotation parameter a , the rotating non-Kerr metric has a deformation parameter which denotes deviations from the Kerr geometry. It is interesting that there are no restrictions on the values of the rotation parameter a and the deformation parameter ϵ . For the rotating non-Kerr black hole, the radius of horizon depends on the polar angular coordinate θ and the spacetime is free of closed timelike curves outside of the outer horizon [6]. If the black hole is more prolate than a Kerr black hole (i.e., $\epsilon > 0$), there exist two disconnected spherical horizons for high rotation parameter, but there is no horizon for $a > M$. If the black hole is more oblate than a Kerr black hole (i.e., $\epsilon < 0$), the horizon always exists for the arbitrary a and the topology of the horizon becomes toroidal [7, 9]. Moreover, in the weak field approximation, such a black hole possesses the same asymptotic behaviors of the usual Kerr black hole in general relativity [6]. Motivated by testing gravity in the strong field region, a lot of efforts has been recently dedicated to the study of the rotating non-Kerr black hole[5–7, 9–12].

It is well known that the accretion processes is a powerful indicator of the physical nature of the central celestial objects, which means that the analysis of the signatures of the accretion disk around the rotating non-Kerr black hole could help us to detect gravity effects in the strong field regime in which general relativity breaks down. The accretion disk is such a structure formed by the diffuse material in orbital motion around a central compact body, which now is an important research topic in the astrophysics. The steady-state thin

accretion disk model is the simplest theoretical model of the accretion disks, in which the disk has negligible thickness so that the heat generated by stress and dynamic friction in the disk can be dispersed through the radiation over its surface [13–16]. This cooling mechanism ensures that the disk can be in hydrodynamical equilibrium and the mass accretion rate in the disk maintains a constant, which is independent of time variable. The physical properties of matter forming a thin accretion disk in a variety of background spacetimes have been investigated extensively in [17–28]. The special signatures appeared in the energy flux and the emission spectrum emitted by the disk can provide us not only the information about black holes in the Universe, but also the profound verification of alternative theories of gravity. The marginally stable orbit for the particle and the conversion efficiency of the central object converting rest mass into outgoing radiation have been studied in the background of a rotating non-Kerr black hole [6, 10], which tells us that with the increase of the deformed parameter ϵ , the marginally stable orbit radius r_{ms} decreases and the conversion efficiency increases. However, the effects of the deformation parameter on the energy flux, the radiation temperature, the spectra luminosity and the spectra cut-off frequency is still open. The main purpose of the present paper is to study the properties of the thin accretion disk in the rotating non-Kerr black hole spacetime and see whether it can leave us the signature of the deformation parameter in the energy flux and the emission spectrum emitted in the mass accretion process.

The paper is organized as follows: in the following section we will review briefly the rotating no-Kerr black hole metric proposed by Johannsen *et al* [6] to test gravity in the strong field regime, and then present the geodesic equations for the timelike particles moving in the equatorial plane in this background. In Sec.III, we study the physical properties of the thin accretion disk around the rotating no-Kerr black hole and probe the effects of the deformation parameter on the energy flux, temperature and emission spectrum of the thin accretion disks onto this black hole. We end the paper with a summary.

II. THE GEODESIC EQUATIONS IN THE ROTATING NON-KERR BLACK HOLE SPACETIME

Let us now review briefly the rotating no-Kerr black hole metric, which is proposed by Johannsen *et al* [6] to test gravity in the strong field regime. Starting from a deformed Schwarzschild solution and applying the Newman-Janis transformation, they constructed a deformed Kerr-like metric which describes a stationary, axisymmetric, and asymptotically flat vacuum spacetime. However, it is not a solution in any known gravity theory. In the standard Boyer-Lindquist coordinates, the metric of this rotating no-Kerr black hole has a form

[6]

$$ds^2 = g_{tt}dt^2 + g_{rr}dr^2 + g_{\theta\theta}d\theta^2 + g_{\phi\phi}d\phi^2 + 2g_{t\phi}dtd\phi, \quad (1)$$

where

$$\begin{aligned} g_{tt} &= -\left(1 - \frac{2Mr}{\rho^2}\right)(1+h), & g_{t\phi} &= -\frac{2aMr \sin^2 \theta}{\rho^2}(1+h), \\ g_{rr} &= \frac{\rho^2(1+h)}{\Delta^2 + a^2 h \sin^2 \theta}, & g_{\theta\theta} &= \rho^2, \\ g_{\phi\phi} &= \sin^2 \theta \left[r^2 + a^2 + \frac{2a^2 Mr \sin^2 \theta}{\rho^2} \right] + \frac{a^2(\rho^2 + 2Mr) \sin^4 \theta}{\rho^2} h, \end{aligned} \quad (2)$$

with

$$\rho^2 = r^2 + a^2 \cos^2 \theta, \quad \Delta = r^2 - 2Mr + a^2, \quad h = \frac{\epsilon M^3 r}{\rho^4}. \quad (3)$$

The constant ϵ is the deformed parameter. The quantity $\epsilon > 0$ or $\epsilon < 0$ corresponds to the cases in which the compact object is more prolate or oblate than a Kerr black hole, respectively. As $\epsilon = 0$, the black hole is reduced to the usual Kerr black hole in General Relativity. The horizon of the black hole is given by [7, 9]

$$\Delta + a^2 h \sin^2 \theta = 0. \quad (4)$$

Clearly, the radius of horizon depends on θ , which is different from that in the usual Kerr case. For the case $\epsilon > 0$, one can find that there exist two disconnected spherical horizons for high spin parameters, but there is no horizon for $a > M$. However, for $\epsilon < 0$ one can find that the horizon never disappears for the arbitrary a and the shape of the horizon becomes toroidal [7, 9]. Moreover, one can find that it is free of closed timelike curves and then causality is satisfied outside of the event horizon [6].

According to the thin accretion disk model, one can assume that the disk is on the equatorial plane and that the matter moves on nearly geodesic circular orbits. In the rotating non-Kerr black hole spacetime (1), the timelike geodesics equations of a particle can be expressed as

$$u^t = \frac{dt}{d\lambda} = \frac{\tilde{E}g_{\phi\phi} - \tilde{L}g_{t\phi}}{g_{t\phi}^2 - g_{tt}g_{\phi\phi}}, \quad (5)$$

$$u^\phi = \frac{d\phi}{d\lambda} = \frac{\tilde{E}g_{t\phi} + \tilde{L}g_{tt}}{g_{t\phi}^2 - g_{tt}g_{\phi\phi}}, \quad (6)$$

$$g_{rr} \left(\frac{dr}{d\lambda} \right)^2 + g_{\theta\theta} \left(\frac{d\theta}{d\lambda} \right)^2 = V_{eff}, \quad (7)$$

with the effective potential

$$V_{eff} = \frac{\tilde{E}^2 g_{\phi\phi} + 2\tilde{E}\tilde{L}g_{t\phi} + \tilde{L}^2 g_{tt}}{g_{t\phi}^2 - g_{tt}g_{\phi\phi}} - 1, \quad (8)$$

where \tilde{E} and \tilde{L} are the specific energy and the specific angular momentum of the particle, respectively.

The circular equatorial orbits obey the conditions $V_{eff} = 0$, $V_{eff,r} = 0$ and $V_{eff,\theta} = 0$ [26–28]. Due to the reflection symmetry of the metric (1) with respect to the equatorial plane, one can find that the condition $V_{eff,\theta} = 0$ is satisfied naturally for the particles locating at the plane $\theta = \pi/2$. Making use of these conditions, we can get the specific energy \tilde{E} , the specific angular momentum \tilde{L} , and the angular velocity Ω of the particle moving in circular orbit on the equatorial plane in the rotating non-Kerr black hole spacetime

$$\tilde{E} = -\frac{g_{tt} + g_{t\phi}\Omega}{\sqrt{g_{tt} - 2g_{t\phi}\Omega - g_{\phi\phi}\Omega^2}} \quad (9)$$

$$\tilde{L} = \frac{g_{t\phi} + g_{\phi\phi}\Omega}{\sqrt{g_{tt} - 2g_{t\phi}\Omega - g_{\phi\phi}\Omega^2}}, \quad (10)$$

$$\Omega = \frac{d\phi}{dt} = \frac{-g_{t\phi,r} + \sqrt{g_{t\phi,r}^2 - g_{tt,r}g_{\phi\phi,r}}}{g_{\phi\phi,r}}. \quad (11)$$

The circular orbits are stable under small perturbations in the radial direction if $V_{eff,rr} \leq 0$, and in the vertical direction if $V_{eff,\theta\theta} \leq 0$ [26–28]. In the background of a Kerr black hole in general relativity, the second condition is always satisfied, so one can obtain the radius of the innermost stable circular orbit by solving $V_{eff,rr} = 0$. However, in the rotating black hole beyond general relativity, the marginally stable orbit radius is determined by the condition $V_{eff,rr} = 0$ or $V_{eff,\theta\theta} = 0$ [26–28]. Unfortunately, in a rotating non-Kerr black hole (1), one can not obtain an analytical form of the marginally stable orbit radius from these conditions. In order to get the marginally stable orbit radius, we must resort to numerical method. In Fig.(1), we set $M = 1$ and plotted the variety of the marginally stable orbit radius r_{ms} with the deformed parameter ϵ in the rotating non-Kerr black hole spacetime. When the black hole is oblate than a Kerr black hole ($\epsilon < 0$), one can find that the radius r_{ms} decreases with the deformed parameter ϵ and the rotation parameter a , which is similar that in the Kerr black hole spacetime. This is also shown in [6]. When the black hole is prolate ($\epsilon > 0$), the dependence of the marginally stable orbit radius r_{ms} on the deformed parameter ϵ becomes more complicated. Let us now first to discuss the case where the particle rotates in the same direction to this prolate black hole ($a > 0$). As the parameter $\epsilon < \epsilon_{c1}$, the marginally stable orbit radius r_{ms} is defined by the radial instability as in the oblate black hole case and r_{ms} decreases with the deformed parameter ϵ . As $\epsilon_{c1} < \epsilon < \epsilon_{c2}$, there are two disconnected regimes where stable circular orbits exist: an outer zone with $r > r_1$ and an inner zone with $r_3 < r < r_2$. Since the energy and angular momentum of the orbit in the inner zone are higher than that in the outer zone, an object inspiraling from large distances on a circular equatorial orbit will reach r_1 and plunge into the central body, rather than finding itself in the inner range of circular orbits. This means that the marginally stable orbit radius r_{ms} is consistent with r_1 , which is defined by the

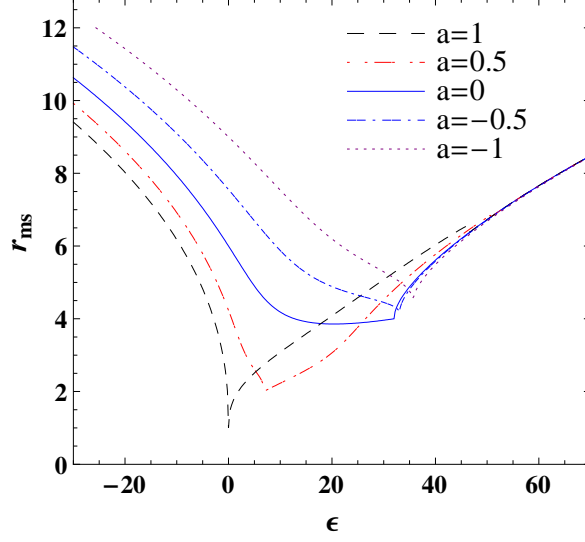


FIG. 1: Variety of the marginally stable orbit radius r_{ms} with the parameter ϵ for the thin disk around the rapidly-rotating non-Kerr black hole.

a	0	0.3	0.5	0.8	1.0
ϵ_{c1}	31.9	28.9	6.9	0.91	0
ϵ_{c2}	∞	51.61	50.73	48.54	46.51
a	-0.3	-0.5	-0.8	-0.9	-1.0
ϵ_{c3}	32.40	33.06	34.50	35.07	35.67

TABLE I: The change of the critical values ϵ_{c1} , ϵ_{c2} , and ϵ_{c3} with the rotation parameter a . Here we set $M = 1$.

vertical instability. One can see that in this regime the marginally stable orbit radius r_{ms} increases with ϵ . Those properties of r_{ms} are similar to those of in the Manko-Novikov metric [27, 28]. As $\epsilon > \epsilon_{c2}$, the outer zone is connected with the inner zone. However, the energy and angular momentum of the orbit are positive and real only if $r > r_4$. Thus, the effective marginally stable orbit is at r_4 and increases with ϵ , which is different from that in the background of a Manko-Novikov spacetime [27, 28]. Moreover, we also find that the effective marginally stable orbit radius r_4 is independent of a for the larger ϵ . The critical values of ϵ_{c1} and ϵ_{c2} are listed in the Table (1) for different rotation parameter a . It is shown that both ϵ_{1c} and ϵ_{2c} decrease with a . For the particle rotating in the opposite direction to the black hole ($a < 0$), we find as the deformed parameter ϵ is less than a certain critical value ϵ_{c3} , the marginally stable orbit radius is defined by the radial instability as in the previous discussion, which r_{ms} decreases monotonously with ϵ . As $\epsilon > \epsilon_{c3}$, we find that only in the region where the energy and angular momentum of the orbit are positive and real, the orbit is

stable under small perturbations both in the radial direction and in the vertical direction since both of the conditions $V_{eff,rr} \leq 0$ and $V_{eff,\theta\theta} \leq 0$ are satisfied. Thus, the effective marginally stable orbit is still at r_4 . The upper bound ϵ_{c3} increases with the absolute value of a as is shown in Table (1). Moreover, we note that for the value of ϵ is much larger than ϵ_{c2} for $a > 0$ and than ϵ_{c3} for $a < 0$, the marginally stable orbit radius is independent of the rotation parameter a .

III. THE PROPERTIES OF THIN ACCRETION DISKS IN THE ROTATING NON-KERR BLACK HOLE SPACETIME

We are now in position to study the accretion process in the thin disk around the rotating non-Kerr black hole and probe how the deformed parameter ϵ affects the energy flux, the conversion efficiency, the radiation temperature and the spectra of the disk in this background. In the thin accretion disk model, the central plane of the disk is assumed to be located in the equatorial plane of the black hole and the disk height H (the maximum half thickness of the disk) is much smaller than the characteristic radius r of the disk, i.e., $H \ll r$. The thin disk can stay in hydrodynamical equilibrium because the heat generated by stress and dynamic friction in the disk can be dispersed through the radiation over its surface. This radiation transport also makes the disk stabilize its thin vertical size. For simplification, we here assume that the thin disk around the rotating non-Kerr black hole is modeled by a steady state accretion disk [15, 16] in which the mass accretion rate \dot{M}_0 stays a constant that does not change with time. In doing so, we can measure the physical quantities of the disk by averaging over a characteristic time scale Δt , the azimuthal angle $\Delta\phi = 2\pi$, and the height H of the disk. In the steady-state accretion disk models, the accreting matter in the disk can be described by an anisotropic fluid with the energy-momentum tensor [15, 16]

$$T^{\mu\nu} = \varepsilon_0 u^\mu u^\nu + 2u^{(\mu} q^{\nu)} + t^{\mu\nu}, \quad (12)$$

where the quantities ε_0 , q^μ and $t^{\mu\nu}$ denotes the rest mass density, the energy flow vector and the stress tensor of the accreting matter, respectively, which are defined in the averaged rest-frame of the orbiting particle with four-velocity u^μ . In the averaged rest-frame, we have $u_\mu q^\mu = 0$ and $u_\mu t^{\mu\nu} = 0$ since both q^μ and $t^{\mu\nu}$ is orthogonal to u^μ [15, 16].

In background of the rotating non-Kerr black hole, one can find that the time-averaged radial structure

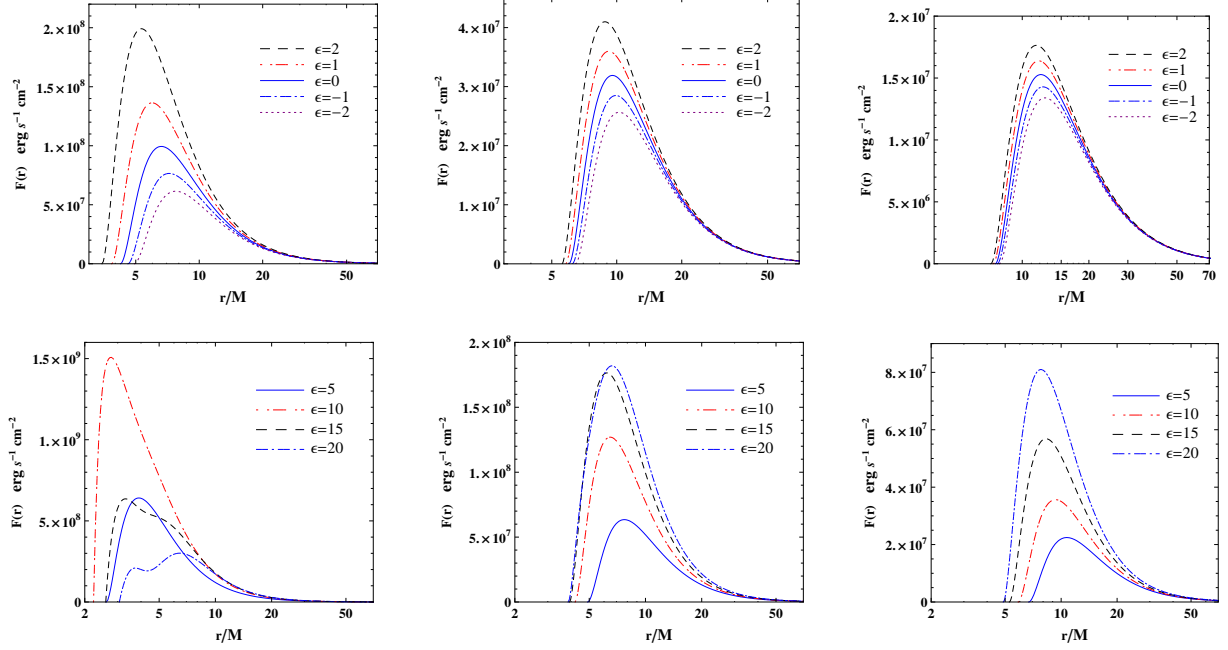


FIG. 2: Variety of the energy flux $F(r)$ with the deformed parameter ϵ in the thin disk around the rotating non-Kerr black hole. The two panels at the left, middle and right correspond to the cases when $a = 0.5$, $a = 0$ and $a = -0.5$, respectively. Here, we set the total mass of the black hole $M = 10^6 M_\odot$ and the mass accretion rate $\dot{M}_0 = 10^{-12} M_\odot \text{ yr}^{-1}$.

equations of the thin disk can be expressed as

$$\dot{M}_0 = -\frac{2\pi(r^3 + \epsilon)}{r^2} \Sigma(r) u^r = \text{Const}, \quad (13)$$

$$\left[\dot{M}_0 \tilde{E} - \frac{2\pi(r^3 + \epsilon)}{r^2} \Omega W_\phi^r \right]_{,r} = \frac{2\pi(r^3 + \epsilon)}{r^2} F(r) \tilde{E}, \quad (14)$$

$$\left[\dot{M}_0 \tilde{L} - \frac{2\pi(r^3 + \epsilon)}{r^2} W_\phi^r \right]_{,r} = \frac{2\pi(r^3 + \epsilon)}{r^2} F(r) \tilde{L}, \quad (15)$$

with

$$\Sigma(r) = \int_{-H}^H \langle \varepsilon_0 \rangle dz, \quad W_\phi^r = \int_{-H}^H \langle t_\phi^r \rangle dz, \quad (16)$$

where $\Sigma(r)$ and W_ϕ^r are the averaged rest mass density and the averaged torque, respectively. The quantity $\langle t_\phi^r \rangle$ is the average value of the $\phi - r$ component of the stress tensor over a characteristic time scale Δt and the azimuthal angle $\Delta\phi = 2\pi$. With the energy-angular momentum relation for circular geodesic orbits $\tilde{E}_{,r} = \Omega \tilde{L}_{,r}$, one can eliminate W_ϕ^r from Eqs.(14) and (15), and then obtain the expression of the energy flux in the mass accretion process

$$F(r) = -\frac{\dot{M}_0 r^2}{4\pi(r^3 + \epsilon)} \frac{\Omega_{,r}}{(\tilde{E} - \Omega \tilde{L})^2} \int_{r_{ms}}^r (\tilde{E} - \Omega \tilde{L}) \Omega_{,r} dr. \quad (17)$$

Here, we consider the mass accretion driven by black holes with a total mass of $M = 10^6 M_\odot$, and with a

mass accretion rate of $\dot{M}_0 = 10^{-12} M_\odot \text{ yr}^{-1}$ [17]. In Fig. (2), we plotted the total energy flux $F(r)$ radiated by a thin disk around the rotating non-Kerr black hole for different deformed parameter ϵ and rotation parameter a . When the black hole is oblate than a Kerr black hole ($\epsilon < 0$), one can find that the energy flux $F(r)$ increases with the deformed parameter ϵ and the rotation parameter a , which is similar to that in the Kerr black hole spacetime. When the black hole is prolate ($\epsilon > 0$), the situation becomes more complex. As $a < 0$, the flux $F(r)$ increases with ϵ for $\epsilon < \epsilon_{c3}$ and decreases with ϵ for $\epsilon > \epsilon_{c3}$. As $a > 0$, we find that with the increase of ϵ , $F(r)$ increases as $\epsilon < \epsilon_{c1}$ and decreases as $\epsilon > \epsilon_{c1}$. Comparing with the behavior of r_{ms} , one can obtain that the dependence of $F(r)$ on ϵ is converse to those of r_{ms} , which can be explained by a fact that the larger r_{ms} enhances the lower limit of integral in the energy flux (17). With the increase of ϵ , the position of the peak value of $F(r)$ moves along the left for the smaller ϵ and moves along right for the larger ϵ . When $\epsilon > \epsilon_{c1}$, the multi-peak value appears in the energy flux $F(r)$. Moreover, we also find that the difference in the energy flux originating from the parameter ϵ increases with the rotation parameter a as $\epsilon < \epsilon_{c2}$ for $a > 0$ and $\epsilon < \epsilon_{c3}$ for $a < 0$. This means that in this region as the black hole rotates more rapidly, the effect of the deformed parameter ϵ on the energy flux $F(r)$ becomes more distinct for the prograde particles and more tiny for the retrograde ones. When $\epsilon > \epsilon_{c2}$ for $a > 0$ and $\epsilon > \epsilon_{c3}$ for $a < 0$, the difference in the energy flux originating from the rotation parameter a vanishes gradually with the increase of ϵ because r_{ms} does not depend on a for the larger ϵ in this region.

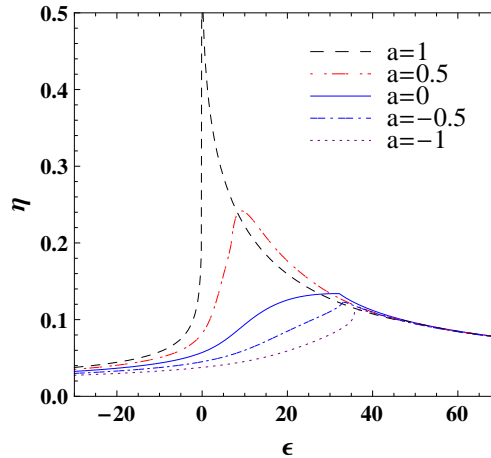


FIG. 3: Variety of the efficient η with the parameter ϵ for the thin disk around the rotating non-Kerr black hole.

In the mass accretion process around a black hole, the conversion efficiency is an important characteristic quantity which describes the capability of the central object converting rest mass into outgoing radiation. In general, the conversion efficiency can be given by the ratio of two rates measured at infinity [14, 15]: the rate

of the radiation energy of photons escaping from the disk surface to infinity and the mass-energy transfer rate of the central compact object in the mass accretion. If all the emitted photons can escape to infinity, one can find that the efficiency η is determined by the specific energy of a particle at the marginally stable orbit r_{ms}

$$\eta = 1 - \tilde{E}_{ms}. \quad (18)$$

The dependence of the conversion efficiency η on the deformed parameter ϵ is plotted in Fig.(3), which shows that when $\epsilon < \epsilon_{c3}$ for $a < 0$ and $\epsilon < \epsilon_{c1}$ for $a > 0$, the larger values of ϵ leads to a much larger efficiency η . This means that in this parameter region the conversion efficiency of the thin accretion disk in the prolate non-Kerr black hole spacetime is more than that in the oblate one. However, as $\epsilon > \epsilon_{c3}$ for $a < 0$ and $\epsilon > \epsilon_{c1}$ for $a > 0$, we find that efficiency η decreases with ϵ . Similarly, for the larger positive ϵ , the conversion efficiency is dominated by the deformed parameter ϵ and independent of the rotation parameter a of the central object. The relationship between the rotation parameter a and deformation parameter ϵ for fixed conversion efficiency η has been discussed in [10].

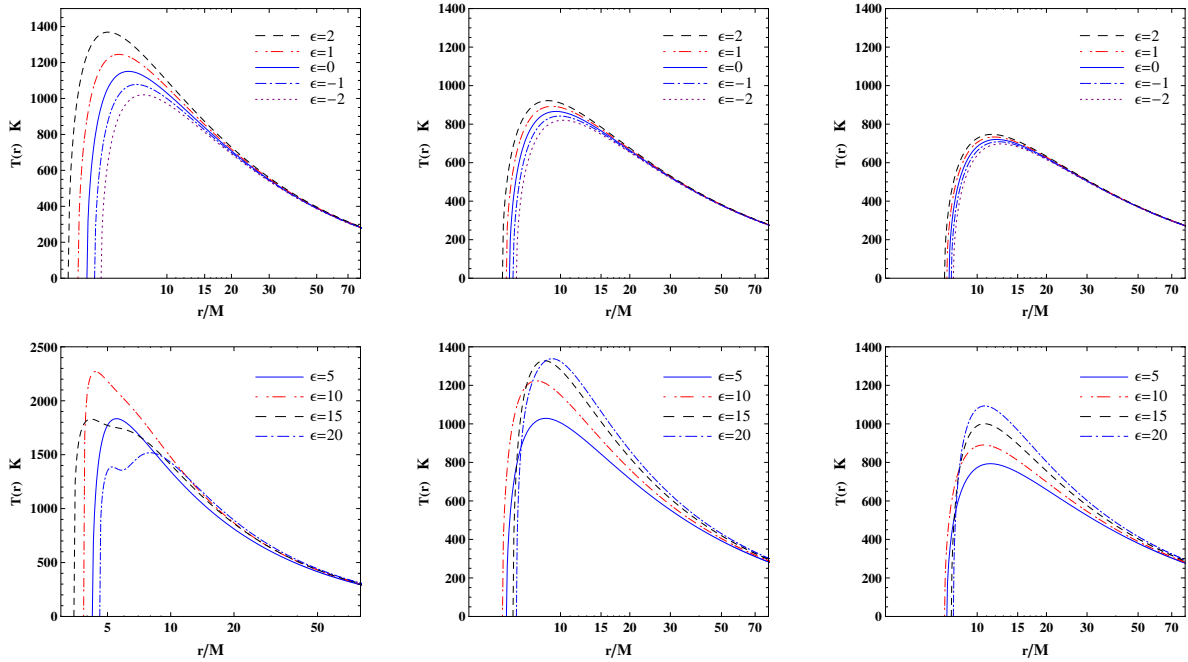


FIG. 4: Variety of the temperature T with the deformed parameter ϵ in the thin disk around the rotating non-Kerr black hole. The two panels at the left, middle and right correspond to the cases when $a = 0.5$, $a = 0$ and $a = -0.5$, respectively. Here, we set the total mass of the black hole $M = 10^6 M_\odot$ and the mass accretion rate $\dot{M}_0 = 10^{-12} M_\odot \text{ yr}^{-1}$.

Let us now to probe the effects of ϵ on the radiation temperature and the spectra of the disk around the rotating non-Kerr black hole. In the steady-state thin disk model [15, 16], it is assumed generally that the accreting matter is in thermodynamic equilibrium, which means that the radiation emitted by the disk surface

can be considered as a perfect black body radiation. The radiation temperature $T(r)$ of the disk is related to the energy flux $F(r)$ through the expression $T(r) = [F(r)/\sigma]^{1/4}$, where σ is the Stefan-Boltzmann constant. This means that the dependence of $T(r)$ on ϵ is similar to that of the energy flux $F(r)$ on ϵ , which is also shown in Fig.(4). Repeating the operations in [20], one can find that the observed luminosity $L(\nu)$ for the thin accretion disk around the rotating non-Kerr black hole can be expressed as

$$L(\nu) = 4\pi d^2 I(\nu) = \frac{16\pi^2 h \cos \gamma}{c^2} \int_{r_i}^{r_f} \frac{\nu^3 (r^3 + \epsilon)}{r^2} \frac{dr}{e^{h\nu/KT(r)} - 1}, \quad (19)$$

where d is the distance to the source, $I(\nu)$ is the thermal energy flux radiated by the disk, and γ is the disk

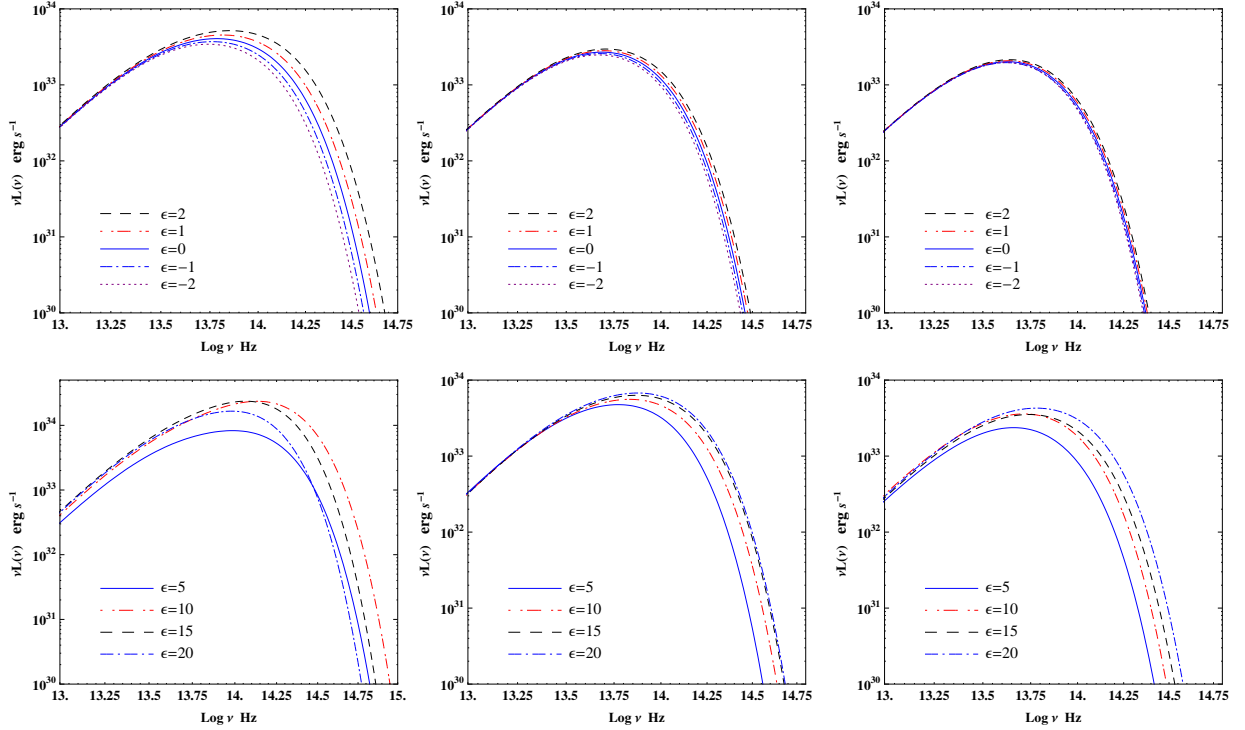


FIG. 5: Variety of the emission spectrum with the deformed parameter ϵ in the thin disk around the rotating non-Kerr black hole. The two panels at the left, middle and right correspond to the cases when $a = 0.5$, $a = 0$ and $a = -0.5$, respectively. Here, we set the total mass of the black hole $M = 10^6 M_\odot$ and the mass accretion rate $\dot{M}_0 = 10^{-12} M_\odot \text{ yr}^{-1}$.

inclination angle. The quantities r_f and r_i are the outer and inner border of the disk, respectively. In order to calculate the luminosity $L(\nu)$ of the disk, we choose $r_i = r_{ms}$ and $r_f \rightarrow \infty$ since the flux over the disk surface vanishes at $r_f \rightarrow \infty$ in the rotating non-Kerr black hole spacetime. Resorting to numerical method, we calculate the integral (19) and present the spectral energy distribution of the disk radiation in Fig.(5). As $\epsilon < \epsilon_{c3}$ for $a < 0$ and $\epsilon < \epsilon_{c1}$ for $a > 0$, we find that the larger value of ϵ leads to the higher cut-off frequencies and the higher observed luminosity of the disk. Moreover, we also find that in this parameter regime the effect of the deformed parameter ϵ on the spectra becomes more distinct for the prograde particles and more tiny

for the retrograde ones. As $\epsilon > \epsilon_{c3}$ for $a < 0$ and $\epsilon > \epsilon_{c1}$ for $a > 0$, both the luminosity and cut-off frequencies decrease with ϵ . Like in the energy flux $F(r)$, the effect of the rotation parameter a on disk spectra vanishes gradually with the increase of ϵ in this region.

IV. SUMMARY

A four-dimensional rotating black hole was proposed recently by Johannsen *et al* [6] to test gravity in the strong field regime. This black hole deviates from the usual Kerr black hole with a deformed parameter and an unbound rotation parameter. The study of such a rotating non-Kerr black hole can help us to understand more deeply about the no-hair theorem and the cosmic censorship conjecture in the strong gravity field regime. In this paper, we have studied the properties of the thin accretion disk in the rotating non-Kerr black hole background. Our results show that the deformed parameter ϵ imprints in the energy flux, temperature distribution and emission spectra of the disk. For the case in which the black hole is more oblate than a Kerr black hole, the large deviation diminishes the energy flux, the conversion efficiency, the radiation temperature, the spectra luminosity and cut-off frequency of the thin accretion disk. For the black hole with positive ϵ , we find that these physical quantities of disk increases with ϵ in the range of $a < 0$ with $\epsilon < \epsilon_{c3}$ and of $a > 0$ with $\epsilon < \epsilon_{c1}$. For the rapidly rotating black hole, the effect of the deformed parameter ϵ on the physical quantities of the thin disk becomes more distinct for the prograde particles and more tiny for the retrograde ones. However, for the cases the parameters located in the range of $a < 0$ with $\epsilon > \epsilon_{c3}$ and of $a > 0$ with $\epsilon > \epsilon_{c1}$, the situation is converse. The energy flux, the conversion efficiency, the radiation temperature, the spectra luminosity and cut-off frequency of the disk decrease with ϵ and the effect originating from the rotation parameter a vanishes gradually with the increase of ϵ . These significant features, at least in principle, may provide a possibility to test gravity in the strong field regime in the future astronomical observations.

V. ACKNOWLEDGMENTS

We would like to thank Prof. C. Bambi for his useful comments and discussions. This work was partially supported by the National Natural Science Foundation of China under Grant No.10875041, the NCET under Grant No.10-0165, the PCSIRT under Grant No. IRT0964 and the construct program of key disciplines in Hunan Province. J. Jing's work was partially supported by the National Natural Science Foundation of China

under Grant Nos. 10875040 and 10935013; 973 Program Grant No. 2010CB833004.

-
- [1] W. Israel, Phys. Rev. **164** (1967) 1776; W. Israel, Commun. Math. Phys. **8** (1968) 245; B. Carter, Phys. Rev. Lett. **26** (1971) 331; S. W. Hawking, Commun. Math. Phys. **25** (1972) 152; D. C. Robinson, Phys. Rev. Lett. **34** (1975) 905.
 - [2] R. Penrose, Riv. Nuovo Cim. Numero Speciale **1** (1969) 252.
 - [3] E. Barausse, V. Cardoso, G. Khanna, Phys. Rev. Lett. **105** (2010) 261102.
 - [4] C. M. Will, Living Rev. Rel. **9** (2005) 3.
 - [5] F. Caravelli, L. Modesto, Class. Quant. Grav. **27** (2010) 24502.
 - [6] T. Johannsen, D. Psaltis, Phys. Rev. D **83** (2011) 12401.
 - [7] C. Bambi, L. Modesto, arXiv:1107.4337 [gr-qc].
 - [8] E. T. Newman and A. I. Janis, J. Math. Phys. **6** (1965) 915 (1965); S. P. Drake and P. Szekeres, Gen. Rel. Grav. **32** (2000) 445.
 - [9] C. Bambi, L. Modesto, arXiv:1110.2768 [gr-qc].
 - [10] C. Bambi, arXiv:1110.0687[gr-qc].
 - [11] P. Pani, C. F. B. Macedo, L. C. B. Crispino, V. Cardoso, arXiv:1109.3996 [gr-qc].
 - [12] T. Johannsen, arXiv:1105.5645v1 [astro-ph.HE].
 - [13] N. I. Shakura and R. A. Sunyaev, Astron. Astrophys. **24** (1973) 33.
 - [14] I. D. Novikov and K. S. Thorne, in Black Holes, ed. C. DeWitt and B. DeWitt, New York: Gordon and Breach (1973).
 - [15] D. N. Page and K. S. Thorne, Astrophys. J. **191** (1974) 499.
 - [16] K. S. Thorne, Astrophys. J. **191** (1974) 507.
 - [17] T. Harko, Z. Kovacs and F. S. N. Lobo, Class. Quant. Grav. **27** (2010) 105010; Phys. Rev. D **80** (2009) 044021; Phys. Rev. D **78**(2008) 084005; Phys. Rev. D **79** (2009) 064001; Class. Quant. Grav. **26** (2009) 215006.
 - [18] S. Bhattacharyya, A. V. Thampan and I. Bombaci, Astron. Astrophys. **372** (2001) 925.
 - [19] Z. Kovacs, K. S. Cheng and T. Harko, Astron. Astrophys. **500** (2009) 621.
 - [20] D. Torres, Nucl. Phys. B **626** (2002) 377.
 - [21] Y. F. Yuan, R. Narayan and M. J. Rees, Astrophys. J. **606** (2004) 1112.
 - [22] F. S. Guzman, Phys. Rev. D **73** (2006) 021501.
 - [23] C. S. J. Pun, Z. Kovacs and T. Harko, Phys. Rev. D **78**, 084015 (2008); Phys. Rev. D **78** (2008) 024043.
 - [24] S. Chen and J. Jing, Phys. Lett. B **704** (2011) 641.
 - [25] Z. Kovacs, L. Gergely and P. Biermann, Mon. Not. Royal Astron. Soc. **416** (2011) 991.
 - [26] C. Bambi and E. Barausse, Astrophys. J. **731** (2011) 121.
 - [27] C. Bambi and E. Barausse, Phys. Rev. D **84** (2011) 084034
 - [28] J. Gair, C. Li and I. Mandel, Phys. Rev. D **77** (2008) 024035